catalysts

MDPI

Article

Novel Magnetically-Recyclable, Nitrogen-Doped Fe_3O_4@Pd NPs for Suzuki–Miyaura Coupling and Their Application in the Synthesis of Crizotinib

Kai Zheng [1], Chao Shen [1,2,*], Jun Qiao [2,*], Jianying Tong [2], Jianzhong Jin [2] and Pengfei Zhang [3]

1 School of Chemistry and Environmental Engineering, Jiangsu University of Technology, Changzhou 213001, China; zkai86@163.com
2 College of Biology and Environmental Engineering, Zhejiang Shuren University, Hangzhou 310015, China; tjy132@msn.com (J.T.); hzjjz@163.com (J.J.)
3 College of Material Chemistry and Chemical Engineering, Hangzhou Normal University, Hangzhou 310036, China; pfzhang@hznu.edu.cn
* Correspondence: shenchaozju@163.com (C.S.); workhard84@126.com (J.Q.); Tel.: +86-0571-88297172 (C.S.); +86-0571-88297103 (J.Q.)

Received: 5 September 2018; Accepted: 22 September 2018; Published: 10 October 2018

Abstract: Novel magnetically recyclable Fe_3O_4@Pd nanoparticles (NPs) were favorably synthesized by fixing palladium on the surface of nitrogen-doped magnetic nanocomposites. These catalysts were fully characterized by Fourier-transform infrared spectroscopy (FTIR), X-ray diffraction (XRD), transmission electron microscopy (TEM), thermogravimetric analysis (TG), and X-ray photoelectron spectroscopy (XPS). The prepared catalyst exhibited good catalytic activity for Suzuki–Miyaura coupling reactions of aryl or heteroaryl halides (I, Br, Cl) with arylboronic acids. These as-prepared catalysts could be readily isolated from the reaction liquid by an external magnet and reused at least ten times with excellent yields achieved. In addition, using this protocol, the marketed drug crizotinib (anti-tumor) could be easily synthesized.

Keywords: heterogeneous catalyst; magnetically; palladium catalysts; nitrogen-doped; Suzuki coupling; crizotinib

1. Introduction

Catalysts are gaining increasing importance, due to their effective manner of solving energy and resource problems, which have become an important part of achieving sustainable development strategies in the 21st century [1,2]. Among the noble metals, palladium and nickel are the most useful catalysts for the formation of C–C bonds in organic transformations [3–5]. In the past, homogeneous Pd catalysts made significant progress in Suzuki–Miyaura coupling reactions; however, it is difficult to separate the products and reuse them. To overcome the drawbacks of homogeneous catalysts, heterogeneous catalysts were significantly explored [6–10]. Heterogeneous catalysis has some advantages such as a recyclable catalytic systems, nontoxic ligands, and a lower amount of palladium residues in products [11–14]. The recovery of Pd catalysts from reaction systems is not easy, and attempts to solve the problem were made by immobilizing the active metal species on supports, such as carbon, silica, metal oxide, polymer, and nanocomposites [15–20]. The magnetic core/shell-supported catalyst is an excellent solution, and its intrinsic magnetic properties enable the efficient separation of the catalysts from the reaction system with an external magnetic field [21,22]. For example, Kumar et al. reported the use of Fe_3O_4@C/Pd as an excellent catalyst for the hydrogenation of aromatic nitro compounds, Suzuki coupling, and sequential reactions; the reactions worked well and gave excellent yields [23]. Sun and coworkers found that the magnetic Fe_3O_4@C/Pd

catalyst showed high catalytic activity for the yield of biphenyl, and it could maintain 90% activity even after being recycled ten times [24]. Fang et al. demonstrated that magnetic Fe_3O_4@C/Pd microsphere catalysts were active in Suzuki coupling [25].

Nitrogen-doped carbon has attracted much attention due to its special structure, good properties, and potential applications [26–30]. Zhang et al. reported that Pd@C–N's high catalytic performance is attributed to the unique structure of the catalytic support–metal and support–substrate junctions. Wang's group found that an as-synthesized Pd/N–carbon nanotube (CNT) catalyst showed high catalytic activity in the Heck reaction, and that the catalyst could be reused at least five times in the aerobic oxidation of benzyl alcohol [31,32]. Movahed and coworkers demonstrated that the good reactivity of the Pd NP–high nitrogen-doped graphene (HNG) catalyst in Suzuki coupling was attributed to the high degree of nitrogen loading in graphene sheets [33].

Continuing our longstanding interest in developing novel carbohydrate-derived catalysts for C–C or C–S coupling reactions [34–38], we were interested in developing a green and efficient chemistry protocol for C–C coupling reactions and related practical applications. Herein, we describe the efficient synthesis of a magnetically-recyclable, nitrogen-doped Fe_3O_4@Pd catalyst for the Suzuki coupling of aryl or heteroaryl halides (I, Br, Cl) with arylboronic acids. These as-prepared catalysts could be easily isolated from the reaction mixture using an external magnet, and they could be reused at least ten times with excellent yields achieved. In addition, the marketed drug crizotinib (anti-tumor) could be easily synthesized using this protocol.

2. Results and Discussion

The preparation procedures of Fe_3O_4@C/Pd and Fe_3O_4@NC/Pd involve three steps, as shown in Scheme 1. Initially, the Fe_3O_4 particles were prepared via a robust solvothermal reaction based on the high-temperature reduction of $FeCl_3 \cdot 6H_2O$ in ethylene glycol [39]. Then, a thin carbon layer was modified with ethylenediamine (EDA) by stirring a mixture of Fe_3O_4, glucose, and EDA in water. The mixture was coated on the surface of the magnetite Fe_3O_4 particles via carbonization under hydrothermal conditions [40]. Ultimately, the Fe_3O_4@NC/Pd and Fe_3O_4@C/Pd catalysts were obtained upon adding $PdCl_2$ to Fe_3O_4@NC or Fe_3O_4@C in ethanol, followed by ascorbic-acid reduction, to generate Pd(0) nanoparticles.

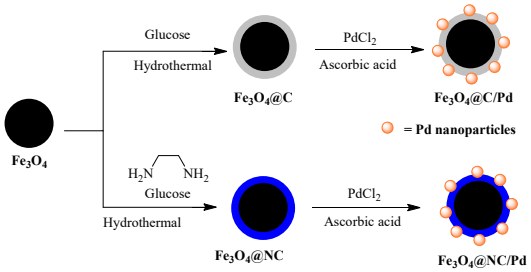

Scheme 1. Synthesis of Fe_3O_4@C/Pd and Fe_3O_4@NC/Pd catalysts.

These as-prepared catalysts were characterized by infrared analysis (FT-IR), thermogravimetric analysis (TG), transmission electron microscopy (TEM), X-ray photoelectron spectroscopy (XPS), X-ray diffraction (XRD) and inductively coupled plasma-optical emission spectrometry (ICP-OES). In Figure 1, the presence of absorption bands at 673 cm^{-1} could correspond to the absorption band of Fe–O and 1336 cm^{-1} could correspond to the O–H bending vibrations; 1558 cm^{-1} and 3386 cm^{-1} are associated with the C=O and O–H vibrations, which confirms the successful attachment of nitrogen-doped carbon on the surface of Fe_3O_4. This also reflects the carbonization of aminated glucose during the hydrothermal process and suggests the presence of large amounts of hydrophilic groups on the Fe_3O_4@NC [41]. The FTIR spectra of Fe_3O_4@NC/Pd (c) and Fe_3O_4@NC (b) were similar to Fe_3O_4 (a), however the FTIR spectra of Fe_3O_4@C/Pd and Fe_3O_4@NC/Pd were different (Figure S1).

The existence of absorption bands at 1382 cm^{-1} (C–H) and 1250 cm^{-1} (C–O) confirmed the arylide was adsorbed by Fe_3O_4@NC/Pd catalyst after the catalytic reaction (Figure S2).

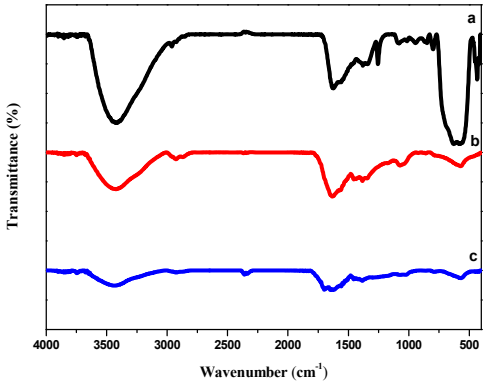

Figure 1. Fourier-transform infrared (FTIR) spectra of (a) Fe_3O_4, (b) Fe_3O_4@NC, and (c) Fe_3O_4@NC/Pd.

The thermal stability of Fe_3O_4 (a), Fe_3O_4@NC (b) and Fe_3O_4@NC/Pd (c) was then proved by TG analysis. Figure 2 shows that catalysts were stable up to 250 °C and suggests that their high thermal stability allows them to be compatible with most organic reactions.

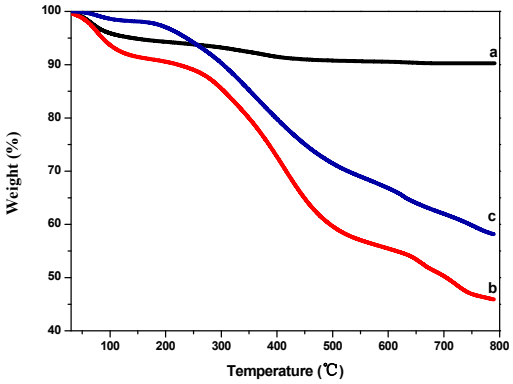

Figure 2. Thermogravimetric analysis graphs of (a) Fe_3O_4; (b) Fe_3O_4@NC; (c) Fe_3O_4@NC/Pd.

The TEM image of Fe_3O_4@NC/Pd is shown in Figure 3. These microspheres essentially have a typical core/shell nanostructure and the average diameter of the catalyst was about 300 nm. The final morphology of Fe_3O_4@NC and Fe_3O_4@C shows a core–shell feature with Pd uniformly deposited on the surface. The TEM studies confirmed the incorporated Pd NPs on the surface of Fe_3O_4@NC nanospheres and also indicated that the catalyst had a core–shell nanostructure. In addition, the results mean the carbonization did not damage the core–shell structure.

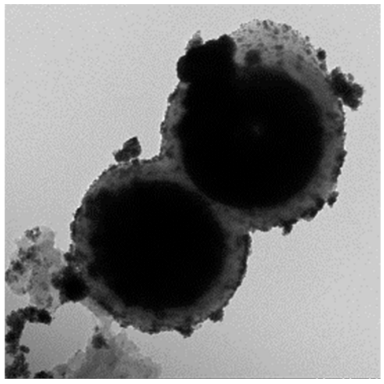

Figure 3. TEM images of Fe_3O_4@NC/Pd catalyst.

As shown in Figure 4, the electronic properties of the Fe_3O_4@NC/Pd catalyst were probed by XPS analysis. As shown in Figure 4a, the peaks corresponding to C1s, N 1s, O 1s, and Pd 3s, 3p and 3d were clearly observed in the XPS survey spectroscopy. This indicates that the nitrogen successfully doped the Fe_3O_4@Pd NPs. The C1s peak of Fe_3O_4@NC/Pd catalyst is shown in Figure 4b. The main peak at 281.1 eV was associated with the C–C, implying that most of the carbon atoms in the Fe_3O_4@NC/Pd catalyst were arranged in a conjugated honeycomb lattice. As shown in Figure 4c, the binding energy of Pd $3d_{3/2}$ and Pd $3d_{5/2}$ were 331.1 eV and 336.2 eV, respectively. The two peaks were the characteristic peaks of Pd(0), suggesting that the absorbed Pd(II) was successfully reduced to Pd(0) nanoparticles under ascorbic-acid reduction. By ICP-OES detection, the content of the Pd element loaded on Fe_3O_4@NC/Pd catalyst was found to be 5 wt%.

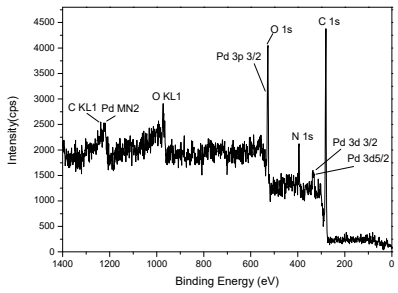

(**a**)

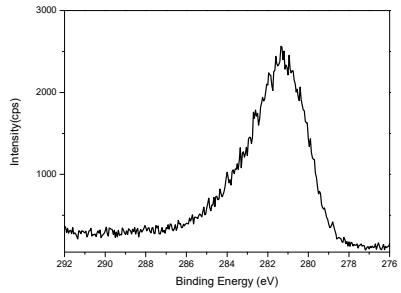

(**b**)

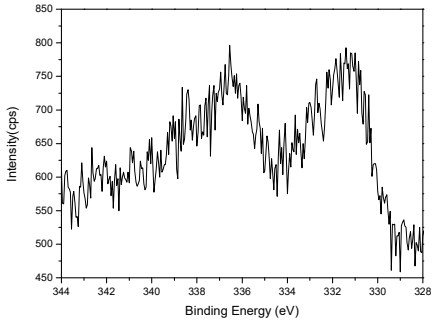

(**c**)

Figure 4. XPS spectra of (**a**) Fe_3O_4@NC/Pd catalyst, (**b**) C 1s and (**c**) Pd 3d.

To evaluate the catalytic performance of these catalysts, Suzuki coupling were carried out as model reactions. The reactions were carried out using water as the solvent and by coupling 4-iodoanisole (1a) with phenylboronic acid (2a), and using different reaction parameters such as the base, the temperature, the time, the dosage and the kind of catalyst to obtain the best reaction conditions. As shown in Table 1, the Fe_3O_4 and the magnetic core–carbon shell were not able to catalyze the reaction (Table 1, entries 1–3). Fe_3O_4@C/Pd and Fe_3O_4@NC/Pd showed good results due to their high reactivity, demonstrating,

respectively, that N-doped carbon has a great influence on the catalytic results, and an increase in the nitrogen loading in carbon sheet leads to an increase in the product yield (Table 1, entries 4, 5). Then, various bases such as K_2CO_3, NaOH, Na_2CO_3, KOH, Et_3N and Cs_2CO_3 were also screened for their effect on the reaction (Table 1, entries 5–10); the best yield was obtained when KOH was used (Table 1, entry 8). Besides, the effect of different temperatures was explored and the results showed that 90 °C was more appropriate for the Suzuki coupling than other temperatures and provided the highest yield of 96% (Table 1, entries 8, 11–14). Next, the effect of the catalyst dosage was examined and the best result was obtained when 10 mg Pd was used as the catalyst (Table 1, entries 8, 16–18). Finally, it was found that the reaction after 0.5 h resulted in a higher yield (Table 1, entries 8, 19–20).

Table 1. Optimization of reaction conditions. [a]

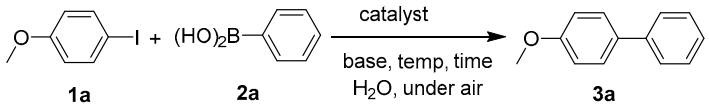

1a **2a** **3a**

Entry	Catalyst (mg)	Base	Temp (°C)	Time (h)	Yield [b] (%)
1	Fe_3O_4	K_2CO_3	90	1	-
2	Fe_3O_4@C	K_2CO_3	90	1	-
3	Fe_3O_4@NC	K_2CO_3	90	1	-
4	Fe_3O_4@C/Pd	K_2CO_3	90	1	84
5	Fe_3O_4@NC/Pd	K_2CO_3	90	1	93
6	Fe_3O_4@NC/Pd	NaOH	90	1	94
7	Fe_3O_4@NC/Pd	Na_2CO_3	90	1	92
8	Fe_3O_4@NC/Pd	KOH	90	1	96
9	Fe_3O_4@NC/Pd	Et_3N	90	1	71
10	Fe_3O_4@NC/Pd	Cs_2CO_3	90	1	83
11	Fe_3O_4@NC/Pd	KOH	rt	1	66
12	Fe_3O_4@NC/Pd	KOH	50	1	75
13	Fe_3O_4@NC/Pd	KOH	70	1	90
14	Fe_3O_4@NC/Pd	KOH	100	1	95
15	Fe_3O_4@NC/Pd	K_2CO_3	50	1	70
16	-	KOH	90	1	-
17	Fe_3O_4@NC/Pd	KOH	90	1	95 [c]
18	Fe_3O_4@NC/Pd	KOH	90	1	77 [d]
19	Fe_3O_4@NC/Pd	KOH	90	0.5	96
20	Fe_3O_4@NC/Pd	KOH	90	0.2	90

[a] The reaction conditions: 4-iodoanisole **1a** (1 mmol), phenylboronic acid **2a** (1.5 mmol), 10 mg catalysts, and base (1.5 mmol) in 3 mL water under air. [b] Isolated yield. [c] 20 mg catalysts. [d] 5 mg catalysts.

After obtaining the optimal reaction conditions, the substrate scope of the aryl halides and arylboronic acids was studied. As shown in Table 2, the effect of different aryl iodides was first carried out using phenylboronic acid (**2a**) as a substrate. The result showed that the substrates with electron-releasing groups gave good yields when compared to electron-withdrawing groups in aryl halides (Table 2, entries 1–13) and meta-substituted or ortho-substituted substrates showed lower yields than the para-substituted arylhalides (Table 2, entries 2,4–7,10–13). These results showed that the steric hindrance and electronic effect of substrates **1a–m** had little effect on the Suzuki coupling under the optimized reaction conditions. Then, the efficiency of the protocol for the Suzuki coupling of aryl bromides or chlorides with corresponding boronic acids was examined. The reaction conditions were quite effective for the coupling of aryl bromides with boronic acids, resulting in high yields (Table 2, entries 14–16). However, only a moderate yield were obtained when aryl chlorides were used as the substrate (Table 2, entries 17–20). The coupling reactions using arylboronic acids were also investigated, and the coupling products were obtained in good yields, the electron-releasing groups in arylboronic acid gave higher yields compared to substrates bearing electron-withdrawing groups (Table 2, entries 21–26). Moreover, the optimized reaction conditions were effective for the Suzuki

coupling of heteroaryl bromides with phenylboronic acids and produced products in satisfactory yields (Table 2, entries 27–32).

Table 2. Suzuki coupling between aryl halides and arylboronic acids in the presence of Fe_3O_4@NC/Pd. [a]

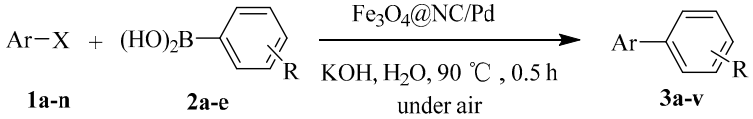

1a-n **2a-e** **3a-v**

Entry	Ar	X	R	Yield [b] (%)
1	4-CH_3O-C_6H_4	I	H	96 (**3a**)
2	4-NH_2-C_6H_4	I	H	96 (**3b**)
3	4-OH-C_6H_4	I	H	97 (**3c**)
4	4-CH_3-C_6H_4	I	H	96 (**3d**)
5	4-NO_2-C_6H_4	I	H	99 (**3e**)
6	4-CHO-C_6H_4	I	H	99 (**3f**)
7	4-$COCH_3$-C_6H_4	I	H	98 (**3g**)
8	4-Cl-C_6H_4	I	H	97 (**3h**)
9	Ph	I	H	97 (**3i**)
10	3-NO_2-C_6H_4	I	H	95 (**3j**)
11	3-$COCH_3$-C_6H_4	I	H	94 (**3k**)
12	2-NH_2-C_6H_4	I	H	88 (**3l**)
13	2-CH_3-C_6H_4	I	H	86 (**3m**)
14	4-CH_3-C_6H_4	Br	H	79 (**3d**)
15	4-CHO-C_6H_4	Br	H	94 (**3f**)
16	Ph	Br	H	94 (**3i**)
17	4-NH_2-C_6H_4	Cl	H	53 [c] (**3b**)
18	4-CHO-C_6H_4	Cl	H	55 [c] (**3f**)
19	4-$COCH_3$-C_6H_4	Cl	H	57 [c] (**3g**)
20	Ph	Cl	H	56 (**3i**)
21	4-CH_3O-C_6H_4	I	4-CHO	98 (**3n**)
22	4-CH_3O-C_6H_4	I	4-OH	97 (**3o**)
23	4-CH_3O-C_6H_4	I	4-CH_3	97 (**3p**)
24	4-CH_3O-C_6H_4	I	4-F	95 (**3q**)
25	4-CH_3O-C_6H_4	I	4-Cl	95 (**3r**)
26	4-CH_3O-C_6H_4	I	3-NO_2	89 (**3s**)
27	2-Py	Br	4-F	85 (**3t**)
28	2-Py	Br	H	88 (**3u**)
29	2-Py	Br	3-NO_2	81 (**3v**)
30	2-quinoline	Br	4-F	82 (**3w**)
31	2-quinoline	Br	H	86 (**3x**)
32	2-quinoline	Br	3-NO_2	80 (**3y**)

[a] The reaction conditions: aryl halides 1 (1 mmol), arylboronic acid 2 (1.5 mmol), Fe_3O_4@NC/Pd catalyst (10 mg), and KOH (1.5 mmol) in water (3 mL) under air. [b] Isolated yield. [c] 8 h.

With this methodology in hand, we turned our attention to the preparation of crizotinib, which is a potent and selective Me-senchymal epithelial factor/anaplastic lymphoma kinase (c-Met/ALK) inhibitor (Scheme 2) [42]. Crizotinib has a palladium residue problem because the aminopyridine coordinates to palladium to form the corresponding stable compounds. As a result, the separation of the crizotinib API from the residual palladium has been a challenging task [43]. Thus, the coupling between aryl bromide **4** and pinacol boronate **5** were carried out employing this method. This transformation was accomplished with excellent results in the presence of the Fe_3O_4@NC/Pd catalyst and KOH in water at 90 °C for 6 h. Then the intermediate **6** was treated with 4 M HCl in 1,4-dioxane/CH_2Cl_2, and the crizotinib API was isolated in very high yield (95%) with >99% purity and <10 ppm Pd.

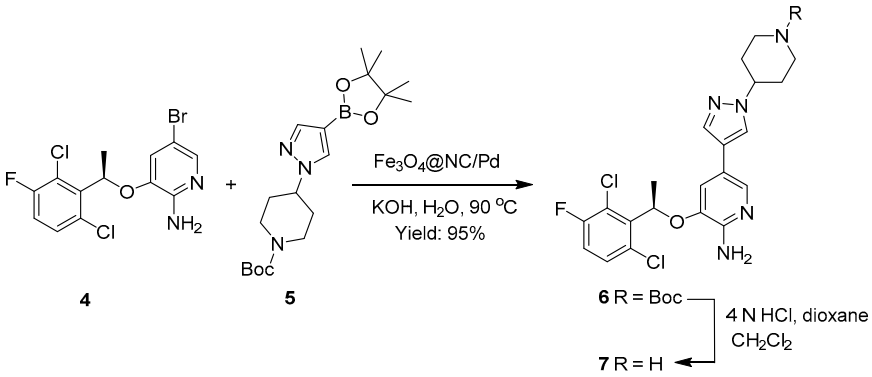

Scheme 2. Application of the catalyst in the synthesis of crizotinib.

The recyclability of the catalyst was then studied using the Suzuki coupling reaction. The reuse experiments for the Fe_3O_4@NC/Pd catalyst were carried out and the catalyst was able to be separated by a permanent magnet after each round and reused in next catalytic reaction. As shown in Figure 5, the magnetic catalyst remained effective and stable after the tenth round, affording a coupling product with 90% yield, which indicated the good stability of the Fe_3O_4@NC/Pd catalyst.

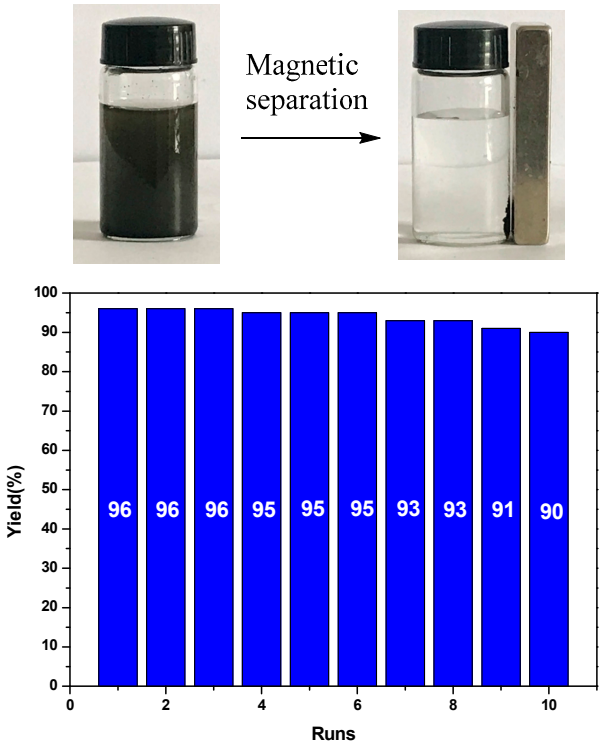

Figure 5. Recycling and reuse of Fe_3O_4@NC/Pd in the Suzuki coupling.

It is well known that using magnetic separation to recycle catalysts is much easier than filtration and centrifugation. A key factor to be investigated is the stability of the catalyst: the leaching of active species into the reaction mixture. When exploring the leaching of Pd from the catalyst, the concentration of Pd in the Fe_3O_4@NC/Pd catalyst was found to be unchanged using ICP-OES analysis. A hot filleting leaching experiment was also conducted. After 0.5 h, the magnetic Fe_3O_4@NC/Pd catalyst was collected by an external magnet, and the clear liquid solution was continuously stirred at 90 °C for 3 h and 2 ppm palladium was determined in the reaction solution, which indicated that there was no leaching of palladium from the catalyst to the reaction solution.

3. Experimental Materials

The starting materials were commercially available and were used without further purification except for the solvents. Ferric chloride hexahydrate ($FeCl_3 \cdot 6H_2O$) was provided by Shanghai Darui Fine Chemicals Co. Ltd (Shanghai, China). Glucose was obtained from Chinasun Specialty Products Co. Ltd (Changshu, China). Sodium acetate anhydrous and ethylene glycol were provided by Shanghai Ling Feng Chemical Reagent Co. Ltd (Shanghai, China). Polyvinyl pyrrolidone (PVP) and ethylenediamine (EDA) were supplied by Aladdin (Shanghai, China). Palladium(II) chloride ($PdCl_2$, 59.5%) was provided by J&K Scientific Ltd (Shanghai, China). Other materials were of analytical grade and used as received.

3.1. Characterization

Fourier-transform infrared (FTIR) spectra were determined with a Bruker Tensor 27 FT-IR (Swiss Brüker, Hangzhou, China) using KBr pellets. Melting points were measured on an X-6 Data microscopic melting point apparatus. Transmission electron microscopy (TEM) images were obtained from a FEI T20 microscope (FEI, Shanghai, China). X-ray diffraction (XRD) measurements were obtained using a Shimadzu XRD-6000 spectrometer (Shimadzu Corp, Beijing, China). X-ray photoelectron spectrographs (XPS) were determined with an Axis Ultra DLD electron spectrometer (Kratos Analytical, Manchester, UK) with the C1s = 284.8 eV signal as the internal standard. The magnetic properties of the catalysts were measured using a vibrating sample magnetometer (VSM) (Lake Shore, New York, NY, USA). Thermogravimetric analyses (TG) were performed with a Q600 simultaneous DSC-TGA (TA Instruments, Shanghai, China) at 20 °C/min in a nitrogen atmosphere (150 mL/min). A total of 10 mg of each sample in an alumina pan was analyzed in the 30–800 °C temperature range. ^1H and ^{13}C NMR spectra were measured with a Bruker Advance 400 spectrometer (Swiss Brüker, Hangzhou, China). by using $CDCl_3$ or DMSO-d_6 as solvents and TMS as the internal standard. The Pd content in the catalyst was measured using a Perkin-Elmer Optima 2100 DV (PerkinElmer, Shanghai, China).

3.2. Preparation of Fe_3O_4 Nanoparticles

Fe_3O_4 nanoparticles were prepared using a solvothermal reaction method [44]. Typically, $FeCl_3 \cdot 6H_2O$ (1.5 g), NaAC (2 g) and PVP (1 g) were dissolved in ethylene glycol (30 mL) under magnetic stirring. The resultant solution was transferred into a Teflon-lined stainless steel autoclave, sealed, and heated to 200 °C for 12 h. After completion of the reaction, the resulting product was separated using an external magnet and washed several times with ethanol water. Finally, the black Fe_3O_4 nanoparticles were dried under vacuum at 60 °C for 24 h.

3.3. Preparation of Fe_3O_4@C Nanoparticles

Fe_3O_4@C was prepared by the in situ carbonization of glucose in the presence of Fe_3O_4 under hydrothermal conditions [45]. Fe_3O_4 nanoparticles (200 mg) were dispersed in water (10 mL) containing glucose (3.2 g) by ultrasonication. Subsequently, it was put into a Teflon lined stainless steel autoclave, sealed, and heated at 180 °C for 10 h and cooled down at room temperature. After completion of the reaction, the resulting nanoparticles were obtained by an external magnet and washed with ethanol followed by water. Finally, the black colored product was dried under vacuum for 24 h to produce Fe_3O_4@C nanoparticles.

3.4. Preparation of Fe_3O_4@NC Nanoparticles

Fe_3O_4@NC was synthesized according to the procedure described in the literature [46]. Fe_3O_4 nanoparticles (100 mg) were first put into 10 mL water containing ethylenediamine (EDA) (0.2 mL) and glucose (1.6 g) and ultrasonicated. Subsequently, the mixture was placed into a Teflon-lined stainless steel autoclave, then the autoclave was sealed and heated at 180 °C for 10 h, before cooling to room temperature. After completion of the reaction, the product was obtained by an external magnet and

washed several times with ethanol and water. Lastly, the black colored product was dried under vacuum for 24 h to provide Fe_3O_4@NC nanoparticles.

3.5. Preparation of the Fe_3O_4@C/Pd and Fe_3O_4@NC/Pd Catalyst

The Fe_3O_4@C/Pd and Fe_3O_4@NC/Pd catalyst were prepared using a published method [45,46]. Typically, the Fe_3O_4@C and Fe_3O_4@NC (400 mg) was well-dispersed in ethanol (40 mL) under ultrasonication for 0.5 h. The resulting black suspension was ultrasonically mixed with $PdCl_2$ (35 mg) ethanol solution (3 mL) for 1 h, then an ascorbic acid ethanol solution (8 mL) was dropped into the above mixture with vigorous stirring under 60 °C. After 2 h of reduction, the products were separated by a permanent magnet and washed several times with water. The products were dried in vacuum to provide Fe_3O_4@C/Pd and Fe_3O_4@NC/Pd.

3.6. General Procedure for the Suzuki Coupling Reactions

Aryl halides (1.0 mmol), arylboronic acid (1.5 mmol), KOH (1.5 mmol), Fe_3O_4@NC/Pd (10 mg) and 3 mL H_2O were put into a reaction flask and stirred at 90 °C under air. After the reaction was complete, the reaction was cooled to room temperature. Then the mixture was extracted with ethyl acetate, dried ($MgSO_4$), filtered, and concentrated in vacuo.

The crude product was purified by column chromatography on silica gel using petroleum/ethyl acetate at 100:1 to afford product.

3.7. General Procedure for Catalyst Recovery

The 4-iodoanisole (1.0 mmol), phenylboronic acid (1.5 mmol), KOH (1.5 mmol), and Fe_3O_4@NC/Pd (10 mg) were mixed in H_2O (3 mL). The mixture was stirred at 90 °C under air. After the completion of the reaction, the catalyst was separated by a permanent magnet and washed with water (3 × 2 mL) and ethanol (3 × 2 mL), then dried in a vacuum and used in the next round.

4. Conclusions

In summary, we developed a novel magnetic Fe_3O_4@NC/Pd, which showed good catalytic activity in the Suzuki coupling of various aryl halides with different arylboronic acids. This catalyst was easily recovered from the reaction by a permanent magnet, and was reused ten times with excellent yields obtained. In addition, this catalyst had high stability, and palladium was hardly ever determined in the reaction solution. Moreover, this catalyst made it easy to synthesize the marketed drug Crizotinib (anti-tumor).

Supplementary Materials: The following are available online at http://www.mdpi.com/2073-4344/8/10/443/s1, Figure S1: FTIR spectra of (a) Fe_3O_4; (b) Fe_3O_4@C; (c) Fe_3O_4@C/Pd, Figure S2: FTIR spectra of (a) fresh Fe_3O_4@NC/Pd and (b) used Fe_3O_4@NC/Pd, Figure S3: Thermogravimetric analysis graphs of (a) Fe_3O_4; (b) Fe_3O_4@C; (c) Fe_3O_4@C/Pd, Figure S4: Thermogravimetric analysis graphs of (a) fresh Fe_3O_4@NC/Pd. and (b) used Fe_3O_4@NC/Pd.

Author Contributions: Conceptualization, C.S. and J.J.; Investigation, K.Z. and J.Q.; Supervision, P.Z.; Writing-original draft, C.S. and J.T.

Funding: This research was funded by Zhejiang Provincial Natural Science Foundation of China (No. LY17B020005), Science and Technology Plan of Zhejiang Province (No. 2017C31054) and the Scientific Research Project of Zhejiang Education Department (No. Y201534569). I acknowledge the support of the Young and Middle-Aged Academic Team Project of Zhejiang Shuren University.

Conflicts of Interest: The authors declare no conflict of interest.

References

1. Li, R.; Zhang, P.; Huang, Y.; Zhang, P.; Zhong, H.; Chen, Q.W. Pd–Fe_3O_4@C hybrid nanoparticles: Preparation, characterization, and their high catalytic activity toward Suzuki coupling reactions. *J. Mater. Chem.* **2012**, *22*, 22750–22755. [CrossRef]

2. Rao, X.; Liu, C.; Zhang, Y.; Gao, Z.; Jin, Z. Pd/C-catalyzed ligand-free and aerobic Suzuki reaction in water. *Chin. J. Catal.* **2014**, *35*, 357–361. [CrossRef]
3. Byum, S.; Chung, J.; Kwon, J.; Kim, B. Mechanistic Studies of Magnetically Recyclable Pd Fe_3O_4 Heterodimeric Nanocrystal-Catalyzed Organic Reactions. *Chem. Asian J.* **2015**, *10*, 982–988.
4. Shi, S.C.; Meng, G.; Szostak, M. Synthesis of Biaryls through Nickel-Catalyzed Suzuki-Miyaura Coupling of Amides by Carbon–Nitrogen Bond Cleavage. *Angew. Chem.* **2016**, *55*, 6959–6963. [CrossRef] [PubMed]
5. Meconi, G.M.; Vummaletis, S.V.C.; Luqueurrutia, J.A.; Belanzoni, P.; Nolan, S.P.; Jacobsen, H.; Cavallo, L.; Sola, M.; Poater, A. Mechanism of the Suzuki–Miyaura Cross-Coupling Reaction Mediated by [Pd(NHC)(allyl)Cl] Precatalysts. *Organometallics* **2017**, *36*, 2088–2095. [CrossRef]
6. Bonis, A.D.; D'Orsi, R.; Funicello, M.; Lupattelli, P.; Santagata, A.; Teghil, R.; Chiummiento, L. First application of homogeneous Pd nanoparticles prepared by pulsed laser ablation in liquid to a Suzuki-type reaction. *Catal. Commun.* **2017**, *100*, 164–168. [CrossRef]
7. Kaboudin, B.; Salemi, H.; Mostafalu, R.; Kazemi, F.; Yokomatsu, T. Pd(II)-β-cyclodextrin complex: Synthesis, characterization and efficient nanocatalyst for the selective Suzuki-Miyaura coupling reaction in water. *J. Organomet. Chem.* **2016**, *818*, 195–199. [CrossRef]
8. Tahmasebi, S.; Mokhtari, J.; Naimi-Jamal, M.R.; Khosravi, A.; Panahi, L. Application of Cu2(BDC)2DABCO Encapsulated Palladium Nanoparticle in Suzuki Coupling. *J. Organomet. Chem.* **2017**, *853*, 35–41. [CrossRef]
9. Chen, Y.; Wang, M.G.; Zhang, L.; Liu, Y.; Han, J. Poly(o-aminothiophenol)-stabilized Pd nanoparticles as efficient heterogenous catalysts for Suzuki cross-coupling reactions. *Rsc. Adv.* **2017**, *7*, 47104–47110. [CrossRef]
10. Mondal, P.; Bhanja, P.; Khatun, R.; Bhaumik, A.; Das, D.; Islam, S.M. Palladium nanoparticles embedded on mesoporous TiO_2 material (Pd@MTiO$_2$) as an efficient heterogeneous catalyst for Suzuki-Coupling reactions in water medium. *J. Colloid Interface Sci.* **2017**, *508*, 378–386. [CrossRef] [PubMed]
11. Yang, P.B.; Ma, Y.; Bian, F.L. Palladium Supported on Metformin-Functionalized Magnetic Polymer Nanocomposites: A Highly Efficient and Reusable Catalyst for the Suzuki–Miyaura Coupling Reaction. *ChemCatChem* **2016**, *8*, 1–24. [CrossRef]
12. Zhang, G.W.; Liu, R.; Chou, Y.J.; Wang, Y.; Cheng, T.Y.; Liu, G.H. Multistep Organic Transformations over Base-Rhodium/Diamine-Bifunctionalized Mesostructured Silica Nanoparticles. *ChemCatChem* **2017**, *9*, 1–8.
13. Hajipour, A.R.; Sadeghi, A.R.; Khorsandi, Z. Pd nanoparticles immobilized on magnetic chitosan as a novel reusable catalyst for green Heck and Suzuki cross-coupling reaction: In water at room temperature. *Appl. Organomet. Chem.* **2017**, *11*, 4112–4122.
14. Chen, J.; Zhang, J.; Zhu, D.J.; Li, T. Porphyrin-based polymer-supported palladium as an excellent and recyclable catalyst for Suzuki–Miyaura coupling reaction in water. *Appl. Organomet. Chem.* **2017**, *8*, 3996–4002. [CrossRef]
15. Fei, S.X.; Han, B.; Li, L.L.; Mei, P.; Zhu, T.; Yang, M.; Chen, H.S. A study on the catalytic hydrogenation of N-ethylcarbazole on the mesoporous Pd/MoO_3 catalyst. *Int. J. Hydrogen Energy* **2017**, *42*, 25942–25950. [CrossRef]
16. Dai, C.Y.; Li, Y.G.; Ning, C.L.; Zhang, W.X.; Wang, X.G. The influence of alumina phases on the performance of Pd/Al_2O_3 catalyst in selective hydrogenation of benzonitrile to benzylamine. *Appl. Catal. A Gen.* **2017**, *545*, 97–103. [CrossRef]
17. Shi, W.; Yu, J.B.; Jiang, Z.J.; Shao, Q.L.; Su, W.K. Encaging palladium(0) in layered double hydroxide: A sustainable catalyst for solvent-free and ligand-free Heck reaction in a ball mill. *Beilstein J. Org. Chem.* **2017**, *13*, 1661–1668. [CrossRef] [PubMed]
18. Celebi, M.; Yurderi, M.; Bulut, A.; Kaya, M.; Zahmakiran, M. Palladium nanoparticles supported on amine-functionalized SiO_2 for the catalytic hexavalent chromium reduction. *Appl. Catal. B Environ.* **2016**, *180*, 53–64. [CrossRef]
19. Hattori, T.; Tsubone, A.; Sawama, Y.; Monguchi, Y.; Sajiki, H. Palladium on Carbon-Catalyzed Suzuki-Miyaura Coupling Reaction Using an Efficient and Continuous Flow System. *Catalysts* **2015**, *5*, 18–25. [CrossRef]
20. Zhang, S.Q.; Li, Y.-R.; Jeon, H.-J.; Ahn, W.-S.; Chung, Y.M. Pd nanoparticles on a microporous covalent triazine polymer for H2 production via formic acid decomposition. *Mater. Lett.* **2018**, *215*, 211–213. [CrossRef]

21. Yang, L.; Jin, Y.Z.; Fang, X.C.; Cheng, Z.M.; Zhou, Z.M. Magnetically Recyclable Core–Shell Structured Pd-Based Catalysts for Semihydrogenation of Phenylacetylene. *Ind. Eng. Chem. Res.* **2017**, *56*, 14182–14191. [CrossRef]
22. Mohammadinezhad, A.; Akhlaghinia, B. Fe_3O_4@ Boehmite-NH_2-Co^{II} NPs: An inexpensive and highly efficient heterogeneous magnetic nanocatalyst for the Suzuki-Miyaura and Heck-Mizoroki cross-coupling reactions. *Green Chem.* **2017**, *19*, 5625–5641. [CrossRef]
23. Kumar, B.S.; Amali, A.J.; Pitchumani, K. Cubical Palladium Nanoparticles on C@Fe_3O_4 for Nitro reduction, Suzuki-Miyaura Coupling and Sequential Reactions. *J. Mol. Catal. Chem.* **2016**, *423*, 511–519. [CrossRef]
24. Sun, C.G.; Sun, K.; Tang, S.K. Extended Stöber method to synthesize core-shell magnetic composite cataly. *Mater. Chem. Phys.* **2018**, *207*, 181–185. [CrossRef]
25. Fang, Q.; Cheng, Q.; Xu, H. Monodisperse magnetic core/shell microspheres with Pd nanoparticles-incorporated-carbon shells. *Dalton Trans.* **2014**, *43*, 2588–2595. [CrossRef] [PubMed]
26. Bolzan, G.R.; Abarca, G.; Goncalves, W.D.G.; Matos, C.F. Imprinted naked Pt nanoparticles on N-doped carbon supports: A synergistic effect between catalyst and support. *M.J.L. Santos J. Dupont Chem. Eur. J.* **2017**, *23*, 1–9. [CrossRef] [PubMed]
27. Ying, J.; Li, J.; Jiang, G.P.; Cano, Z.P.; Ma, Z.; Zhong, C.; Su, D.; Chen, Z.W. Metal-organic frameworks derived platinum-cobalt bimetallic nanoparticles in nitrogen-doped hollow porous carbon capsules as a highly active and durable catalyst for oxygen reduction reaction. *Appl. Catal. B Environ.* **2018**, *225*, 496–503. [CrossRef]
28. Chen, Y.Q.; Li, X.F.; Wei, Z.Z.; Mao, S.J.; Deng, J.; Cao, Y.L.; Wang, Y. Efficient synthesis of ultrafine Pd nanoparticles on an activated N-doping carbon for the decomposition of formic acid. *Catal. Commun.* **2018**, *108*, 55–58. [CrossRef]
29. Wei, Z.Z.; Li, X.F.; Deng, J.; Wang, J.; Li, H.R.; Wang, Y. Improved catalytic activity and stability for hydrogenation of levulinic acid by Ru/N-doped hierarchically porous carbon. *Mol. Catal.* **2018**, *448*, 100–107. [CrossRef]
30. Cao, Y.L.; Mao, S.J.; Li, M.M.; Chen, Y.Q.; Wang, Y. Metal/porous carbon composites for heterogeneous catalysis: Old catalysts with improved performance promoted by N-doping. *ACS Catal.* **2017**, *7*, 8090–8112. [CrossRef]
31. Zhang, P.; Gong, Y.; Li, H.; Chen, Z.; Wang, Y. Selective oxidation of benzene to phenol by $FeCl_3$/mpg-C_3N_4 hybrids. *RSC Adv.* **2013**, *3*, 5121–5126. [CrossRef]
32. Wang, L.L.; Zhu, L.P.; Bing, N.C.; Wang, L.J. Facile green synthesis of Pd/N-doped carbon nanotubes catalysts and their application in Heck reaction and oxidation of benzyl alcohol. *J. Phys. Chem. Solids* **2017**, *107*, 125–130. [CrossRef]
33. Movahed, S.K.; Dabiri, M.; Bazgir, A. Palladium nanoparticle decorated high nitrogen-doped graphene with high catalytic activity for Suzuki–Miyaura and Ullmann-type coupling reactions in aqueous media. *Appl. Catal. A Gen.* **2014**, *488*, 265–274. [CrossRef]
34. Shen, C.; Xu, J.; Yu, W.; Zhang, P. ChemInform Abstract: A Highly Active and Easily Recoverable Chitosan@Copper Catalyst for the C–S Coupling and Its Application in the Synthesis of Zolimidine. *Green Chem.* **2014**, *16*, 3007–3012. [CrossRef]
35. Shen, C.; Shen, H.; Yang, M.; Xia, C.; Zhang, P. Novel D-glucosamine-derived pyridyl-triazole@palladium catalyst for solvent-free Mizoroki-Heck reactions and its application in the synthesis of Axitinib. *Green Chem.* **2014**, *17*, 225–230. [CrossRef]
36. Shen, H.; Shen, C.; Chen, C.; Wang, A.; Zhang, P. Novel glycosyl pyridyl-triazole@palladium nanoparticles: Efficient and recoverable catalysts for C–C cross-coupling reactions. *Catal. Sci. Technol.* **2015**, *5*, 2065–2071. [CrossRef]
37. Shen, C.; Zhang, P.; Sun, Q.; Bai, S.; Andy Hor, T.A.; Liu, X. Recent advances in C–S bond formation via C–H bond functionalization and decarboxylation. *Chem. Soc. Rev.* **2015**, *46*, 291–314. [CrossRef] [PubMed]
38. Ying, B.; Xu, J.; Zhu, X.; Shen, C.; Zhang, P. Inside Cover: Catalyst-Controlled Selectivity in the Synthesis of C_2- and C_3-Sulfonate Esters from Quinoline N-Oxides and Aryl Sulfonyl Chlorides. *ChemCatChem* **2016**, *8*, 2604–2608. [CrossRef]
39. Hameed, R.M.A. A core–shell structured Ni–Co@Pt/C nanocomposite-modified sensor for the voltammetric determination of pseudoephedrine HCl. *New. J. Chem.* **2018**, *42*, 2658–2668. [CrossRef]

40. Zhu, M.; Diao, G. Magnetically Recyclable Pd Nanoparticles Immobilized on Magnetic Fe_3O_4@C Nanocomposites: Preparation, Characterization, and Their Catalytic Activity toward Suzuki and Heck Coupling Reactions. *J. Phys. Chem. C.* **2011**, *115*, 24743–24749. [CrossRef]
41. Sun, L.; Wang, L.; Tian, C.; Tan, T.; Xie, Y.; Shi, K.; Li, M.; Fu, H. Nitrogen-doped graphene with high nitrogen level via a one-step hydrothermal reaction of graphene oxide with urea for superior capacitive energy storage. *RSC. Adv.* **2012**, *2*, 4498–4506. [CrossRef]
42. Magano, J.; Dunetz, J.R. Large-scale applications of transition metal-catalyzed couplings for the synthesis of pharmaceuticals. *Chem. Rev.* **2011**, *111*, 2177–2250. [CrossRef] [PubMed]
43. De Koning, P.D.; McAndrew, D.; Moore, R.; Moses, I.B.; Boyles, D.C.; Kissick, K.; Stanchina, C.L.; Cuthbertson, T.; Kamatani, A.; Rahman, L.; et al. Fit-for-Purpose Development of the Enabling Route to Crizotinib (PF-02341066). *Org. Process Res. Dev.* **2011**, *15*, 1018–1026. [CrossRef]
44. Liu, B.; Ren, Y.; Zhang, Z. Aerobic oxidation of 5-hydroxymethylfurfural into 2,5-furandicarboxylic acid in water under mild conditions. *Green Chem.* **2015**, *17*, 1610–1617. [CrossRef]
45. Kumar, B.S.; Amali, A.J.; Pitchumani, K. Mesoporous Microcapsules through d-Glucose Promoted Hydrothermal Self-Assembly of Colloidal Silica: Reusable Catalytic Containers for Palladium Catalyzed Hydrogenation Reactions. *Appl. Mater. Interfaces* **2015**, *7*, 22907–22917.
46. Liu, Z.Y.; Zhang, C.L.; Luo, L.; Chang, Z.J.; Sun, X.M. One-pot synthesis and catalyst support application of mesoporous N-doped carbonaceous materials. *J. Mater. Chem.* **2012**, *22*, 12149–12154. [CrossRef]